RSC Advances

ROYAL SOCIETY
OF CHEMISTRY

www.rsc.org/advances

Synthesis of *Gum rosin* alcohol-poly(acrylamide) based adsorbent and its application in removal of malachite green dye from waste water

B S Kaith,[*a] Rajeev Jindal,[a] Rachna Sharma[a]

Abstract

The present paper is focused on the synthesis of green GrA-cl-poly(AAm) adsorbent using *N, N'*-methylene-bis-acrylamide and potassium persulphate as crosslinker-initiator system. The synthesized adsorbent was found to remove 83% toxic malachite green dye from aqueous waste water. Kinetic studies of the adsorption of dye on the adsorbent showed pseudo second kinetics and was found to fit well to Langmuir isotherm model.

Keywords: Copolymer, hydrogel, *Gum rosin,* malachite green, adsorption

1.0 Introduction

Hydrogels are three dimensional branched and crosslinked networks which prevent them from dissolution in aqueous medium. They generally contain -OH, $-NH_2$, -COOH, $-CONH_2$ and $-SO_3$ functional groups. Long polymeric chains of hydrogels create larger space within the matrix due to electrostatic repulsion of ionized groups resulting in extensive water, saline or physiological fluid intake.[1-9] Such materials are widely used in agriculture, biomedical, tissue engineering and as sorbents in textile industry for removal of dyes and heavy metal ions.[10-24]

Rosin, also known as resin acids or rosin acids, is a natural gum derived from pine and other conifer trees. It consists of diterpene resin acids with characteristic bulky hydrophenanthrene structures such as abietic, neoabietic, levopimaric and pimaric acids with the empirical formula $C_{19}H_{29}COOH$. It has been found to show excellent biocompatibility and hydrophobicity due to the presence of prominent and unique hydrophenanthrene structure of rosin acids. They are widely used as food additives, paint binders, adhesives, curing agents and as drug carriers.[25-28]

---

[a] *Department of Chemistry, Dr. B.R. Ambedkar National Institute of Technology, Jalandhar, Punjab-144011, India. E-mail: bskaith@yahoo.co.in; Tel.: +91-181-2690301, Ext 2201, 2205, Fax: +91-181-2690932*

Different researchers have worked on such materials and have used them in different applications.[29-32]

Nowadays, various industries such as textiles, leather, plastics, dyestuff and paper, use to drain waste synthetic dyes in nearby water sources and are main sources of water contamination. Even small amounts of organic dyes effect transmission of sunlight into water and disturb biological activity of aquatic life. Removal of such toxic dyes is essential and therefore, polymeric adsorbents with a variety of methods[33] of cleaning waste water are used because of their high efficiency and play an important role in removal of such dyes.[34-54]

As per the literature survey and to the best of our knowledge not much work has been reported on the synthesis of reduced *Gum rosin* based acrylamide grafted hydrogel. Therefore, in the present study synthesis of *Gum rosin*-acrylamide crosslinked hydrogel and its application in the removal of malachite green dye from aqueous medium is reported.

The novelty of present work lies in the conversion of non-biodegradable *Gum rosin* acids mixture into biodegradable and eco-friendly rosin alcohols mixture which further was converted into green crosslinked grafted adsorbent using acrylamide. The synthesized crosslinked adsorbent was found to be of great importance in removal of toxic dyes like malachite green from waste aqueous medium. Hence the device synthesized is of great importance from environment and industrial point of view.

2.0 Experimental

2.1 Material and methods

Gum rosin (Gr) and potassium persulphate (KPS) were procured from Himedia and Sd-Fine Chemicals Pvt. Ltd., respectively. *N, N'*-methylene-bis-acrylamide (MBA) and acrylamide (AAm) were purchased from MERCK.

2.2 Conversion of rosin acids into alcohols

In the reaction flask 6.6 g of *Gum rosin* was dissolved in 100 ml of diethyl ether. It was followed by the slow addition of 4.54 g of $NaBH_4$ dissolved in 40 ml diethyl ether. The reaction mixture was stirred at room temperature overnight and the excess of $NaBH_4$ was destroyed with drop by drop addition of 120 ml methanol. 5% H_2SO_4 solution was used to wash reaction mixture and the organic layer collected was further washed with 5% $NaHCO_3$ solution. Different types of components present in the *Gum rosin* such as abietic acid, neo-abietic acid, palustric, levopimaric, dihydroabietic acid, pimaric, isopimaric and sandaracopimeric got converted into alcoholic form in the presence of $NaBH_4$. After drying over anhydrous Na_2SO_4 and evaporation to dryness a mixture of reduced *Gum rosin* components was obtained.[32]

2.3 Synthesis of GrA-cl-poly(AAm) hydrogel

1.0g *Gum rosin* alcohols was immersed in 4.5ml of deionized water along with a calculated amount of potassium persulphate (0.057 $molL^{-1}$) followed by the addition of acrylamide (2.34 $molL^{-1}$) and N,N'-methylene-bis acrylamide (0.60 $molL^{-1}$) with continuous stirring. Reaction was carried out at a 65^0C temperature and for a fixed time period (2h). Homopolymer was removed with soxhlet extraction using acetone. Graft copolymer obtained was dried in hot air oven at 50°C till a constant weight was obtained. Optimization of various reaction parameters such as solvent amount, polymerization time, temperature, initiator concentration, monomer concentration, crosslinker concentration and pH was carried out as a function of percent swelling.[2]

2.4 Swelling studies

To study the swelling capacity of GrA-cl-poly(AAm) hydrogel, a pre-weighed amount of dry hydrogel was immersed in 100 ml of deionized water at ambient temperature. Weight of swollen sample was taken at regular time intervals and percentage swelling ($\%P_s$) was calculated using following Equation:[10]

$$\%Swelling = \frac{W_{s-}W_d}{W_d} \times 100 \quad \textbf{(1)}$$

Where W_s and W_d are the weights of the swollen and dry samples, respectively.

2.5 Dye removal studies

The adsorption of malachite green (MG) dye was studied by batch experiments. Solutions with varied concentrations ranging from 2-10 ppm were prepared. A known weight of hydrogel sample was placed in 100 ml dye solution and the effects of initial concentration of dye, physiological pH, sample concentration and temperature on adsorption behaviour were studied.

The absorbance of dye solution was measured at 663 nm. The amount of dye adsorbed per unit mass of hydrogel (q_t) was determined using following equation.[35, 45]

$$q_t = \frac{(C_0 - C_t)V}{M} \tag{2}$$

Where, V is volume of the dye solution, M is the mass of dry hydrogel, t refers to the time of treatment.

The percentage dye removal was calculated using the following equation:[35]

$$\%R = \frac{C_0 - C_e}{C_0} \times 100 \tag{3}$$

Where, C_0 and C_e are the initial and equilibrium concentrations of MG dye.

2.6 Instrumental Analysis

FT-IR spectra of backbone and candidate sample were recorded on Agilent Technologies Carry 630 spectrophotometer with a diamond crystal, in the range of 4000-400 cm^{-1} with 4 cm^{-1} resolution. TGA/DTA/DTG studies were carried out in inert atmosphere at a heating rate of 10 ^0C/min within temperature range of 40-750^oC on SII EXSTAR 6000 TGA/DTA thermal analyser. Scanning Electron Micrographs (SEM) were taken on LEO-435VF, LEO Electron Microscopy Ltd. X-ray diffraction analysis (XRD) was performed using XPERT PRO, X-ray diffractometer. Data were obtained at 2θ scale from 10° to 70° at a rate of 1°/min with a step size of 0.02 degree.

Coherence length of the samples was calculated by using Scherrer equation:[55]

$$L = 0.9\lambda / \beta_{½} \text{ x } \cos\theta \tag{4}$$

Where, λ= wavelength, θ = diffraction angle, L = coherence length and $\beta_{½}$ = full width half maximum

3.0 Results and Discussion

3.1 Mechanism

3.1.1 Conversion of Rosin acids into alcohols:

Initially *Gum rosin* acids were converted into alcohols using $NaBH_4$[32] and the reduction of acids into alcohols takes place as per the following reaction (Eq. 5):

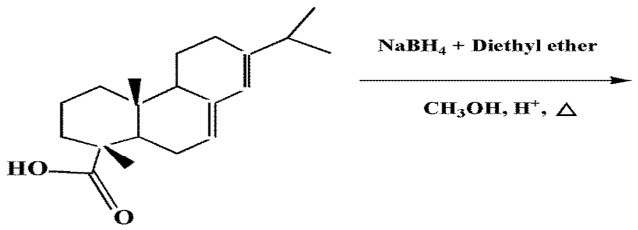

(5)

3.1.2 Grafting of poly(AAm) chains onto reduced backbone:

-CH_2 and –OH are the primary sites for the grafting of poly(vinyl) chains onto backbone along with crosslinking leading to the formation of GrA-cl-poly(AAm). Since potassium persulphate was used as a thermal initiator, therefore, it gets decomposed at reaction temperature and gives rise to SO_4^{-*} (Eq. 6) which further react with water molecules to give rise OH^* (Eq. 7). That OH^* generated active free radical sites on backbone (*Gum rosin* alcohol) (Eq. 8) and monomer (Eq. 9). Live poly(AAm) chains get grafted onto active sites of backbone (Eq. 10) and the formation of graft copolymer takes place (Eq. 10). Different poly(AAm) chains undergo crosslinking with MBA thereby leading to the formation of crosslinked adsorbent GrA-cl-poly(AAm) (Eq. 11).[7, 56, 57]

$$K_2S_2O_8 \xrightarrow{\triangle} 2SO4^{-\bullet} \qquad (6)$$

$$SO_4^{-\bullet} + H_2O \longrightarrow OH^{\bullet} + HSO_4^{-} \qquad (7)$$

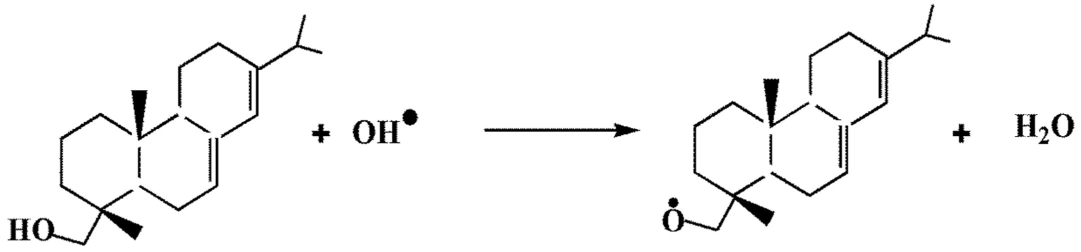

(8)

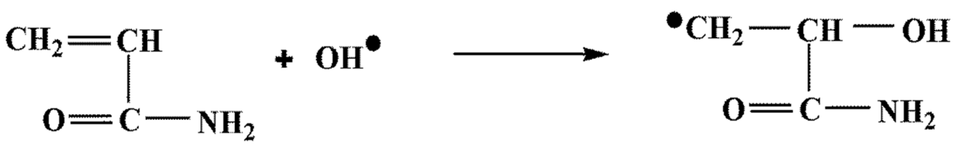

$$\underset{O{=}C{-}NH_2}{CH_2{=}CH} + OH^{\bullet} \longrightarrow {}^{\bullet}CH_2{-}\underset{O{=}C{-}NH_2}{CH}{-}OH \qquad (9)$$

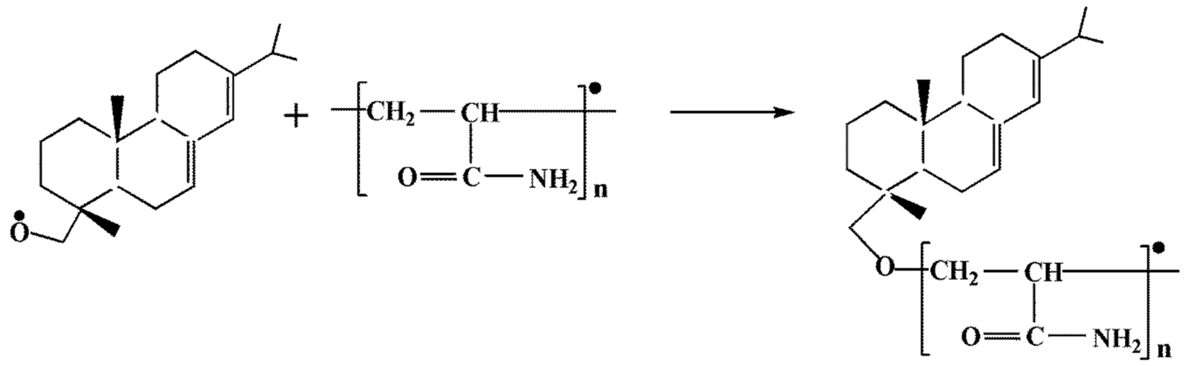

(10)

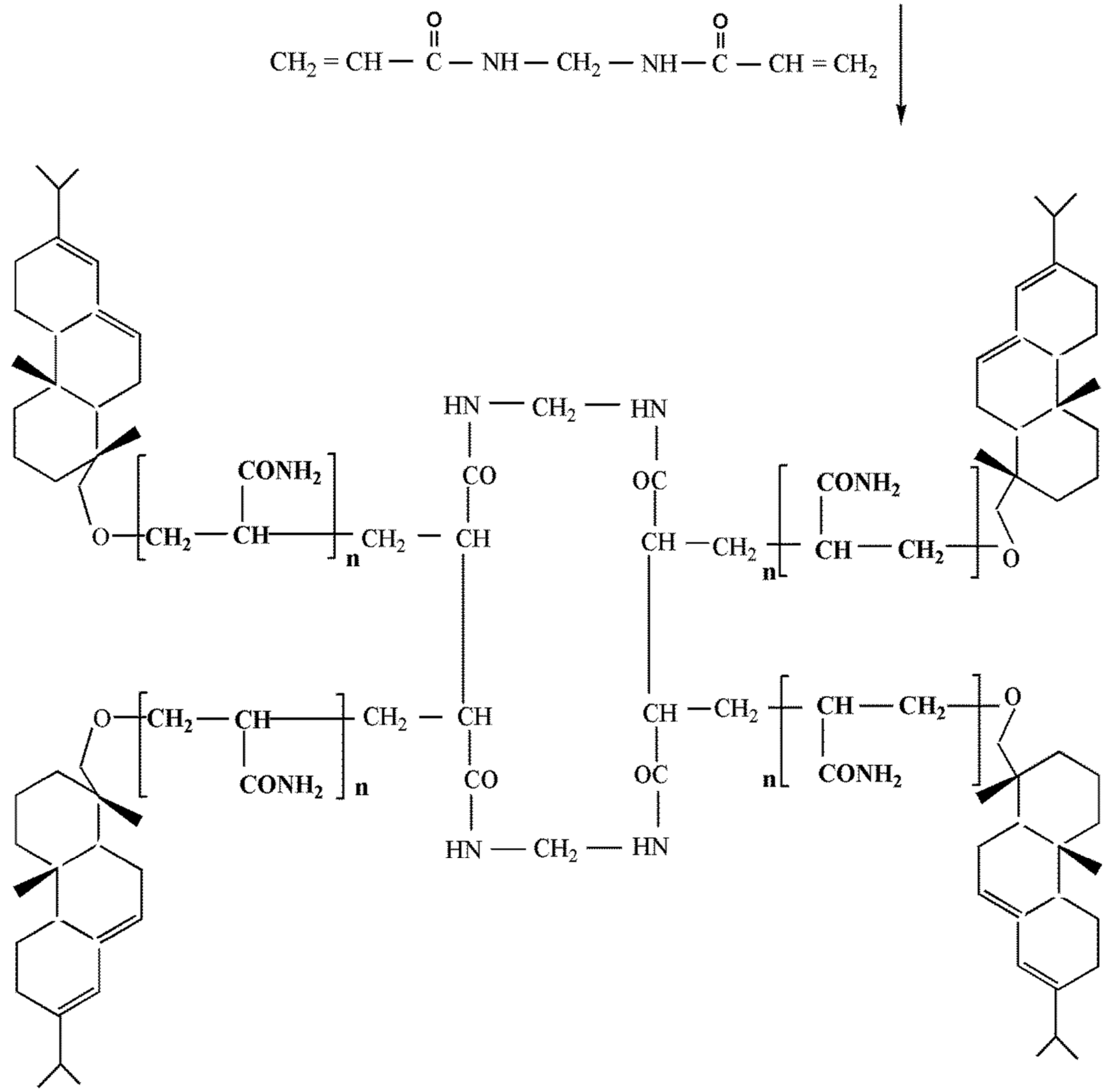

$$CH_2=CH-\overset{O}{\overset{\|}{C}}-NH-CH_2-NH-\overset{O}{\overset{\|}{C}}-CH=CH_2$$

(11)

3.2 Optimization of different reaction parameters

Reaction time and temperature play an important role in deciding the preparation of a device with optimal percentage swelling. Initially the samples showed increase in P_s with increase in reaction time and temperature. Maximum P_s was observed at 120 min interval (P_s = 220%) and at 65^{0}C (P_s =240%). However, further increase in reaction time and temperature resulted in samples with decreased swelling capacity. It may be due to intense crosslinking on increased time interval and temperature resulting in highly crosslinked compact samples with lesser P_s (Table 1).[58]

Initiator and crosslinker concentrations were found to have a significant impact on the P_s of the synthesized samples. Hydrogel synthesized with 0.057 molL^{-1} KPS and 0.60 molL^{-1} MBA showed 188.9% and 200% $P_{s,}$ respectively. Further increase in initiator and crosslinker concentration resulted in decreased swelling, which could be due to over crosslinking and more compactness of the samples with smaller liquid uptake capacity (Table 1).[7]

In case of optimization of acrylamide concentration for getting the samples with maximum P_s (300%) 2.34 molL^{-1} concentration was found to be optimal. Further increase in acrylamide concentration resulted with decreased P_s which could be due to the more rigidness and compactness of the samples (Table 1).[7, 55]

During optimization process physiological pH was found to play an important role in deciding the swelling capacity of the synthesized samples. Samples synthesized under pH 7.0 were found to exhibit maximum liquid uptake capacity (P_s 120%) in comparison to the samples synthesized under acidic and basic conditions. This could be due to the maximum ion – ion repulsions and minimum ion – screening effect at pH 7.0 (Table 1).[2, 58]

Table 1: Optimization of different reaction conditions in the synthesis of GrA-cl-poly(AAm)

Sr. No.	Initiator [mol L^{-1}]	Reaction time (min)	Reaction temperature (^{0}C)	Solvent (ml)	pH of reaction medium	Crosslinker [mol L^{-1}]	Monomer [mol L^{-1}]	Swelling (%)
1	0.040	300	60	**3**	7.0	0.158	3.12	84.62
2	0.040	300	60	**3.5**	7.0	0.158	3.12	100.0
3	0.040	300	60	**4**	7.0	0.158	3.12	115.0
4	0.040	300	60	**4.5**	7.0	0.158	3.12	**160.0**
5	0.040	300	60	**5**	7.0	0.158	3.12	143.5
6	**0.024**	300	60	4.5	7.0	0.158	3.12	125.0
7	**0.032**	300	60	4.5	7.0	0.158	3.12	133.0
8	**0.040**	300	60	4.5	7.0	0.158	3.12	146.7
9	**0.048**	300	60	4.5	7.0	0.158	3.12	172.7
10	**0.056**	300	60	4.5	7.0	0.158	3.12	**188.9**
11	**0.065**	300	60	4.5	7.0	0.158	3.12	137.5
12	**0.073**	300	60	4.5	7.0	0.158	3.12	130.0

13	0.056	300	**50**	4.5	7.0	0.158	3.12	116.7
14	0.056	300	**55**	4.5	7.0	0.158	3.12	121.4
15	0.056	300	**60**	4.5	7.0	0.158	3.12	130.0
16	0.056	300	**65**	4.5	7.0	0.158	3.12	**240.0**
17	0.056	300	**70**	4.5	7.0	0.158	3.12	130.8
18	0.056	**60**	65	4.5	7.0	0.158	3.12	114.3
19	0.056	**120**	65	4.5	7.0	0.158	3.12	**220.0**
20	0.056	**180**	65	4.5	7.0	0.158	3.12	107.7
21	0.056	**240**	65	4.5	7.0	0.158	3.12	100.0
22	0.056	**300**	65	4.5	7.0	0.158	3.12	90.9
23	0.056	120	65	4.5	**3.0**	0.158	3.12	45.5
24	0.056	120	65	4.5	**5.0**	0.158	3.12	62.5
25	0.056	120	65	4.5	**7.0**	0.158	3.12	**122.2**
26	0.056	120	65	4.5	**9.0**	0.158	3.12	90.0
27	0.056	120	65	4.5	**11.0**	0.158	3.12	50.0
28	0.056	120	65	4.5	7.0	**0.014**	3.12	166.7
29	0.056	120	65	4.5	7.0	**0.043**	3.12	**200.0**
30	0.056	120	65	4.5	7.0	**0.086**	3.12	185.7
31	0.056	120	65	4.5	7.0	**0.158**	3.12	162.5
32	0.056	120	65	4.5	7.0	**0.229**	3.12	116.7
33	0.056	120	65	4.5	7.0	0.043	**1.56**	200.0
34	0.056	120	65	4.5	7.0	0.043	**2.34**	**300.0**
35	0.056	120	65	4.5	7.0	0.043	**3.12**	150.0
36	0.056	120	65	4.5	7.0	0.043	**3.9**	130.0
37	0.056	120	65	4.5	7.0	0.043	**4.68**	115.0

3.3 Removal of MG dye from aqueous medium

Synthesized sample GrA-cl-poly(AAm) was evaluated for its efficiency in the removal of MG from water. Different parameters like initial concentration of dye and feed concentrations were optimized in order to get the maximum uptake of dye through the test sample.

3.3.1 Effect of initial concentration of dye

The effect of initial concentration of MG dye was investigated by varying the initial concentration of dye from 2-10 ppm. Dye adsorption experiments were carried out at pH 7.0. It was observed that the dye adsorption through GrA-cl-poly(AAm) increases sharply with increase in the initial dye concentration. Thus, the dye adsorbed per unit mass of hydrogel (q_t) value of 0.3–1.4 mgL^{-1} could result in 72-83% dye removal in the solution concentration range of 2-10 ppm. Malachite green (MG) is cationic dye with tertiary amine groups. The obtained trends can be due to strong electrostatic interaction between functional groups of the GrA-cl-poly(AAm) and dye molecules resulting in high adsorption and removal (Fig. 1). Comparative studies of different adsorbents reported in the literature for the removal of different types of dyes have been depicted in Table 2. It has been observed that the synthesized adsorbent has the dye adsorption capacity almost equal to the reported adsorbents in the literature.[50-54, 59-61] Moreover, the synthesized adsorbent being prepared from natural backbone is eco-friendly and biodegradable in nature which is the advantage over the synthetic adsorbent. The mechanism for the binding of MG dye with the crosslinked graft copolymer is shown in Scheme I. $=N^+(CH_3)_2Cl^-$ group present on the malachite green dye forms a complex with the -NH group of the crosslinked adsorbent through H-bonding, thereby resulting in the removal of dye from waste water.[7]

Table 2: Comparison of adsorption capacity of the GrA-cl-poly(AAm) adsorbent with other adsorbents

Materials	Dose	Dye	Concentration (mg L^{-1})	Adsorption capacity (mg/g)	Reference
Acrylic acid-Acrylamide polymer	Diameter 1.2cm	CV & BM	50	4.12	50
TiO_2/Acrylamide-Acrylic acid polymer	0.2g	MB	5.0	5.0	51
Acrylamide/Lap polymer	1.0g	BB9, BB12, BV1	30	45	52
Poly(AM-DADMAC)/silica sol	0.08g	MO	30	31	53
Poly(AM-HEMA)	0.05g	MV, RB	1.5	0.12	54
Cellulose	0.5g	MG	30-50	0.48-0.79	59
Charcoal	0.01g	MG	4.6	0.180	60
Activated carbon of Ricinus communis	0.02g	MG	50-200	4.8-34.0	61
GrA-cl-poly(AAm)	0.5g	MG	2-10	0.3-1.4	Present study

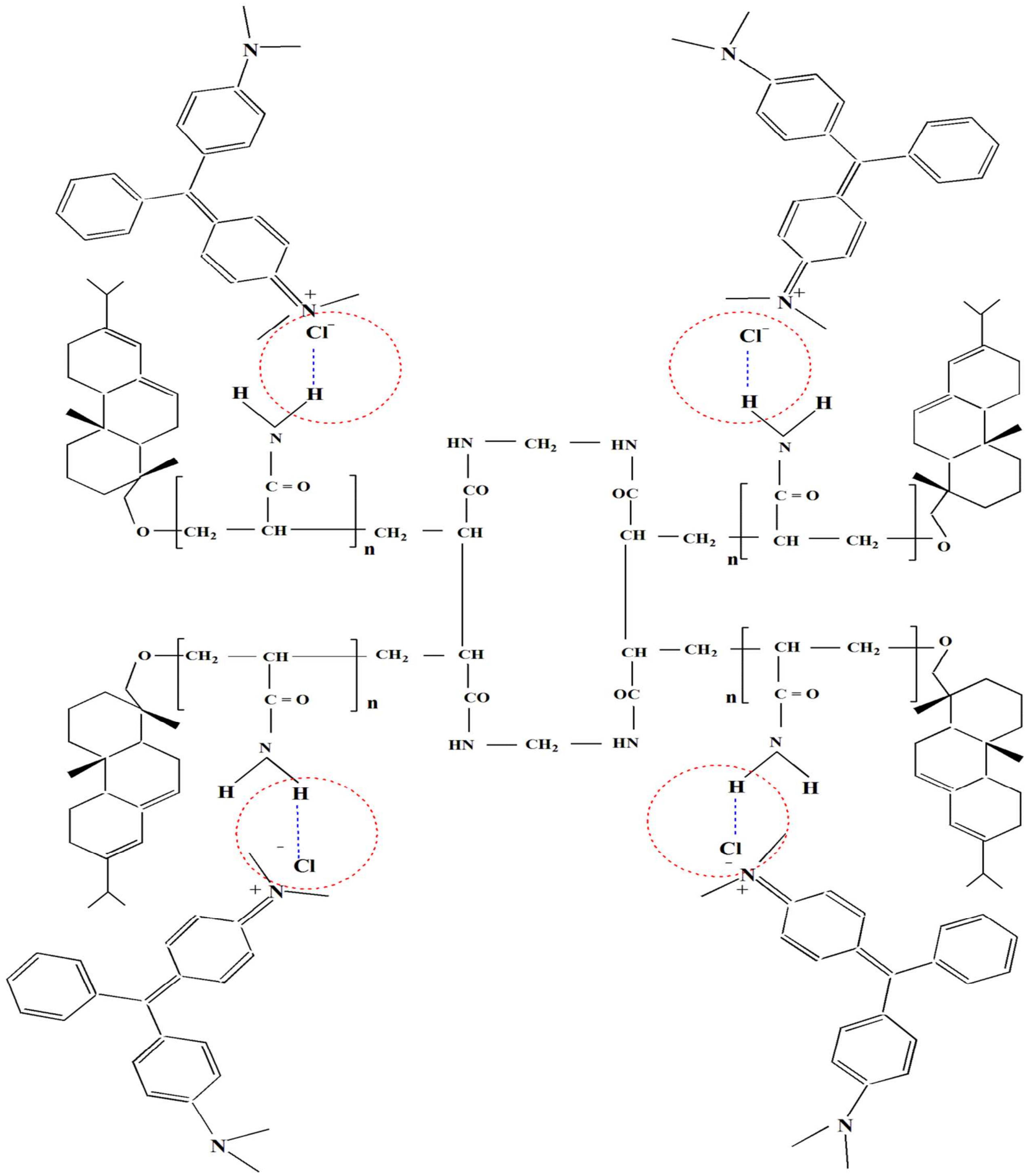

Scheme I Adsorption of MG dye onto GrA-cl-poly(AAm) hydrogel

3.3.2 Effect of feed concentration

The effect of GrA-cl-poly(AAm) dose on the removal of MG dye was observed by using different amounts of sample. Percentage dye removal was found to increase with increase in feed dose. The higher dye removal (83%) was obtained with 500mg dose (Fig. 2). It was observed that the presence of higher amounts of GrA-cl-poly(AAm) provides large number of active adsorbent sites for removal of the dye.[42]

3.4 Dye adsorption kinetics

Adsorption of dye on GrA-cl-poly(AAm) depends on physical and chemical interaction between dye and hydrogel as well as transport of dye from bulk solution to hydrogel surface. The dye adsorption by the hydrogel was evaluated in terms of adsorption kinetics by measuring adsorption at various time intervals (q_t) till equilibrium (q_e) for a fixed initial concentration of MG dye was attained. The kinetics of dye adsorption was determined by pseudo second order equation of Ho and McKay because initial adsorption was found to fit well to this non-linear equation and for evaluating diffusion mechanism intra – particle diffusion equation of Weber and Morris:[41, 45]

$$q_t = \frac{{q_e}^2\, k_2 t}{1 + k_2 q_e t} \tag{12}$$

$$q_t = k_p t^{1/2} + c \tag{13}$$

Where q_t and q_e are dye adsorbed at time t and at equilibrium, respectively. k_2 (g mg^{-1} min^{-1}) is second order rate constant, k_p (mg g^{-1} $min^{-1/2}$) is rate constant for intra particle diffusion and c is intercept which signifies boundary layer resistance. The graph of second order kinetic and intra particle diffusion was shown in (Figs. 3a-b). The various kinetic parameters (q_t, k_2, k_p and c) were determined by directly fitting q_t and t in Eqs. (12) and (13). The obtained values of second-order rate constants and intra-particle diffusion constants k_2, K_p and q_e values are reported in Table 3. The results indicated that the correlation coefficients (R^2) for the second order kinetic model were close to 1.0 for all cases indicated a good fit of the models to the experimental data set. Therefore, the good fitting of MG dye adsorption data to pseudo second order kinetics also confirms chemisorption involving electronic interaction between dye molecules and GrA-cl-poly(AAm) as the rate controlling step.

Table 3: Pseudo-second order kinetic and Intra-particle diffusion constants

Concentration (ppm)	Pseudo-second order kinetic constants		
	k_2 (g mg^{-1} min^{-1})	q_{ecal} (mg g^{-1})	R^2
2	0.0049	0.39	0.998
6	0.1208	0.86	0.997
10	0.3043	1.44	0.997
	Intra-particle diffusion		
	K_p (mg g^{-1} $min^{-1/2}$)	c	R^2
2	0.3552	0.15	0.996
6	0.0748	0.40	0.992
10	0.1184	0.53	0.991

Where, k_2 = second order rate constant; k_p = intra particle diffusion rate constant

3.5 Adsorption isotherm models

The dye adsorption data was directly fitted to the non-linear Langmuir and Freundlich model. Langmuir adsorption isotherm model assumes adsorption at homogeneous sites of GrA-cl-poly(AAm) with negligible interaction among adsorbed dye molecules and is explained as:[42]

$$\boldsymbol{Q_e = \frac{Q_{max}K_LC_e}{1/K_LC_e}} \qquad \textbf{(14)}$$

Where C_e is equilibrium dye concentration, Q_{max} is the monolayer capacity of the adsorbent hydrogel (mg g^{-1}) and K_L is Langmuir equilibrium constant (dm^3 g^{-1}). The constants K_L and Q_{max} values were calculated from the intercept and slope of the linear plot of $1/Q_e$ vs $1/C_e$ (Fig. 4) and the values are tabulated in Table 4.

The shape of the Langmuir isotherm was calculated by the dimensionless constant called separation factor, R_L.

$$\boldsymbol{R_L = \frac{1}{1+ K_LC_i}} \qquad \textbf{(15)}$$

Where C_i is initial concentration of MG dye in water and K_L is Langmuir constant. R_L values indicate the type of isotherm to be linear ($R_L = 1$), irreversible ($R_L = 0$), favorable ($0 < R_L < 1$) or unfavorable ($R_L > 1$).

Freundlich model is obtained by assuming multilayer adsorption with non-uniform distribution of heat of adsorption affinities over the heterogeneous surface and is described by the equation given below:[42]

$$\mathbf{q_e = K_F\, C_e{}^{1/n}} \tag{16}$$

Where K_F (mg g^{-1}) is the adsorption capacity and 1/n is the adsorption intensity. The values of 1/n indicate the type of isotherm to be favorable ($0 < 1/n < 1$), unfavorable ($1/n > 1$) and irreversible ($1/n = 0$). The values of K_F and n were obtained from the intercept and slope of the plot of log q_e vs log C_e and are tabulated in Table 4.

Table 4: Adsorption isotherm studies using Langmuir and Freundlich isotherm models

Temperature (K)	**Langmuir Isotherm**		
	K_L (L mg^{-1})	**$q_{max\ cal}$(mg g^{-1})**	**R^2**
303	0.3601	2.93	0.999
313	0.1849	4.37	0.999
323	0.1421	4.76	0.999
	Freundlich Isotherm		
	K_F (mg g^{-1})	**n**	**R^2**
303	1.349	1.36	0.996
313	1.505	1.29	0.994
323	1.726	1.18	0.997

Where, K_L = Langmuir equilibrium constant; K_F = Adsorption capacity

3.6 Thermodynamic parameters

Thermodynamic parameters such as Gibbs function change (ΔG^0), standard enthalpy change (ΔH^0) and standard entropy change (ΔS^0) were used to obtain temperature dependency of the adsorption process. The value of ΔG^0 may be obtained from the following equation:[40, 45]

$$\Delta G^0 = -RT \ln K_d \tag{17}$$

Where K_d is the thermodynamic equilibrium constant which can be calculated from equilibrium dye adsorption (q_e) and equilibrium dye concentration (C_e):

$$K_d = \frac{q_e}{C_e} \tag{18}$$

The effect of temperature on thermodynamic constant can be calculated as

$$\frac{d \ln K_d}{dT} = \frac{\Delta H^0}{RT^2} \tag{19}$$

Integrating and rearranging Eq. (19) following Eq. (20) was obtained:

$$\ln K_d = -\frac{\Delta H^0}{RT} + \frac{\Delta S^0}{R} \quad (20)$$

The values of ΔH^0 and ΔS^0 were obtained from the slope and intercept of linear plot of ln K_d vs 1/T (Fig. 5) and are tabulated in Table 5. K_d was obtained at different temperature (30, 40, 50, 60 and 70^0C) from dye adsorption at different concentration using Eq. (18). Dye adsorption gradually decreased at higher temperature which indicated exothermic nature of adsorption. The positive values of ΔG^0 at all temperatures indicated that the dye adsorption process is not spontaneous. The decrease in ΔG^0 value with decrease in temperature showed greater dye adsorption at low temperature. The negative value of ΔH^0 confirmed the exothermic nature of dye adsorption process.

Table 5: Thermodynamic analysis at different temperature

Temperature (K)	ln K_d	ΔG^0(KJ mol^{-1})	ΔH^0(KJ mol^{-1})	ΔS^0(KJ mol^{-1})x 10^{-2}	R^2
303	-0.62	1.56	-5.51	-2.33	0.992
313	-0.68	1.78			0.991
323	-0.75	1.99			0.990
333	-0.80	2.22			0.980
343	-0.89	2.54			0.970

Where, K_d = Thermodynamic equilibrium constant; ΔG^0 = Gibbs function; ΔH^0 = Standard enthalpy change; ΔS^0 = Standard entropy change

3.7 Characterization

3.7.1 FTIR

Reduction of *Gum rosin* acids into alcohols was confirmed using FTIR spectroscopy. FTIR spectrum of *Gum rosin* showed broad peak at 2921.63 cm^{-1} which corresponds to -OH stretching of carboxylic acid. Peak at 1689.45 cm^{-1} is assigned to -C=O stretching of carboxylic acid and 1381.81 cm^{-1} is attributed to -C-O stretch of carboxylic acid (Fig. 6a).

On the other hand FTIR spectra of *Gum rosin* alcohols showed a broad peak at 3201.45 cm^{-1} contributing to the -OH stretching of alcohols. Peak at 1409.63 cm^{-1} corresponds to C-C bending and 1185.45 cm^{-1} is assigned to C-O stretch of alcohol. Thus, FTIR spectra confirmed the reduction of the different types of acidic components present in the *Gum rosin* (Fig. 6b).

FTIR spectrum of graft copolymer of acrylamide with reduced *Gum rosin* showed a sharp peak at 3193.27 cm^{-1} corresponding to N-H stretch of amide. Peak at 1655.09 cm^{-1} was due to -C=O stretching of amide I band, at 1471.81 cm^{-1} attributed to N-H in-plane bending of amide II band and 1103.63 cm^{-1} corresponds to C-N stretching vibrations amide III band.[57, 58] Thus, FTIR spectrum confirmed the grafting of acrylamide onto reduced *Gum rosin* (Fig. 6c).

Additional peaks have been found in the FT-IR spectrum of dye adsorbed on crosslinked graft copolymer and showed a peak at 2935.68 cm^{-1} which corresponds to C-H stretching. Peak at 1651.81 cm^{-1} is evidence of the C=C stretching of the benzene rings and peak at 1416.36 cm^{-1} showed C-C stretching in the ring and at 1106.13 cm^{-1} observed was due to aromatic C-N stretching vibrations. The peak at 870.68 cm^{-1} indicated bending of the ring hydrogens. Thus, appearance of additional peaks in the spectra of the sample alongwith the peaks of grafted sample confirmed the adsorption of dye on the grafted adsorbent sample (Fig. 6d).[59, 62]

3.7.2 Scanning electron microscopy

The surface morphology of *Gum rosin,* reduced *Gum rosin* and poly(AAm) grafted reduced *Gum rosin* was studied using SEM technique (Figs. 7a-c). It was observed that the surface of *Gum rosin* was smooth, whereas, the reduced *Gum rosin* showed crystalline and rough morphology. It may be due to alignment of crystallites of *Gum rosin* alcohols after the reduction process.

In case of poly(AAm) chains grafted reduced *Gum rosin*, a rough surface morphology was found which may be due to the incorporation of poly(AAm) chains onto reduced backbone through covalent bonding.[57, 63]

3.7.3 Thermogravimetric analysis

TGA / DTA / DTG techniques were used to study the thermal behaviour of *Gum rosin*, reduced *Gum rosin* and GrA-cl-poly(AAm). In each case, two stage decomposition was found (Table 6). Ist stage decomposition of *Gum rosin*, reduced *Gum rosin* and GrA-cl-poly(AAm) was observed at 237–343.3 ^{0}C, 100.5–416.7 ^{0}C and 104.4–373.3 ^{0}C with 60.3%, 18.4% and 20.9% wt. loss, respectively. Whereas final decomposition of *Gum rosin,* reduced *Gum rosin* and GrA-cl-poly(AAm) was found at 534.3 ^{0}C, 752.4 ^{0}C and 750.3 ^{0}C with second stage decomposition wt.

loss of 33.4%, 7.6% and 34%, respectively. The decomposition below 400 ^{0}C could be due to the breakdown of poly(AAm) chains of grafted samples.[64] Thus, it is clear from the TGA results that GrA-cl-poly(AAm) is thermally more stable than the *Gum rosin* which could be due to the incorporation of poly(AAm) chains onto reduced *Gum rosin* through covalent bonding during the grafting process.[58, 65]

In case of DTA *Gum rosin* was found to show exothermic peak at 493.4 ^{0}C (58.1 µV) whereas reduced *Gum rosin* exhibited two endothermic peaks at 118.9 ^{0}C (-34.8 µV) and 267.6 ^{0}C (-0.9 µV). However, GrA-cl-poly(AAm) was found to give endothermic peak at 109 ^{0}C (-12.8 µV) and exothermic peak at 708.3 ^{0}C (10.1 µV), it represents elimination of residual hydroxyl groups due to disintegration at higher temperature.[66] Thus, the DTA data was found to support the TGA studies.

DTG studies clearly showed that rate of weight loss was minimum in case of GrA-cl-poly(AAm) followed by reduced *Gum rosin* and *Gum rosin* (Table 6). Thus, DTG studies were found on the pattern of TGA and clearly indicates that GrA-cl-poly(AAm) was thermally more stable than the backbone. Significant differences in thermal behaviour between the *Gum rosin,* reduced *Gum rosin* and crosslinked grafted product are associated with the incorporation of poly(AAm) chains onto reduced backbone through covalent bonding and further crosslinking with MBA.[56]

Table 6: Thermal behaviour of *Gum rosin* acids, *Gum rosin* alcohols and semi-IPN

	TGA					DTA		DTG	
Sample code	**IDT (^{o}C)**	**1st stage decomposition (%Wt. Loss)**	**2nd stage decomposition, ^{o}C (%wt. Loss)**	**FDT (^{o}C)**	**Residue left (%)**	**Exo/Endothermic peaks at different decomposition Temperature, ^{o}C (µV)**		**Decomposition temperature, ^{o}C (rate of wt. loss in (mg/min)**	
						1st	**2nd**	**1st**	**2nd**
Gr	237.0	237.0-343.3 ^{o}C (60.3%)	343.3-534.3 ^{o}C (33.4%)	534.3	(0.1%)	493.4 (58.1)	-	301.8 (0.79)	497.1 (0.26)
GrA	100.5	100.5-416.7 ^{o}C (18.4%)	416.7-752.4 ^{o}C (7.6%)	752.4	(73.4%)	118.9 (-34.8)	267.6 (-0.9)	117.0 (0.70)	269.1 (0.15)
GrA-cl-poly(AAm)	104.4	104.4-373.7 ^{o}C (20.9%)	373.7-750.3 ^{o}C (34.0%)	750.3	(39.6%)	109.0 (-12.8)	708.3 (10.1)	108.0 (0.34)	711.0 (0.192)

Where, Gr = *Gum rosin*; GrA = *Gum rosin* alcohols; GrA-cl-poly(AAm) = crosslinked grafted adsorbent

3.7.4 X-Ray Diffraction studies

The XRD patterns of *Gum rosin*, reduced *Gum rosin* and GrA-cl-poly(AAm) are shown in (Fig. 8a-c). In case of *Gum rosin* the main diffused and broad characteristic peak occurred at 15.66^0 and showed amorphous character.[67] Whereas, in case reduced *Gum rosin* sharp peak was obtained at 28.03^0 and exhibited crystalline character. On the other hand, in case of GrA-cl-poly(AAm) characteristic peak occurred at 28.04^0 with reduced intensity which indicated that poly(AAm) chains got grafted onto reduced *Gum rosin* backbone through covalent bonding.[2]

Average crystallite size (L) was found higher in case of reduced *Gum rosin* followed by GrA-cl-poly(AAm) and *Gum rosin* (Table 7). XRD results clearly indicate that amorphous *Gum rosin acids* got transformed into crystalline entity on reduction to *Gum rosin* alcohols.

However, on grafting of poly(AAm) chains onto the mixture of *Gum rosin* alcohols, a semi–crystalline material was obtained. This can be due to the reason that incorporation of poly(AAm) chains onto crystalline backbone resulted in the disturbance of crystalline lattice of the backbone.[7] Because of semi–crystalline nature, the GrA-cl-poly(AAm) showed better dye uptake capacity from the aqueous medium which is of great industrial significance.

Table 7: XRD parameters of *Gum rosin* acids, *Gum rosin* alcohols and semi-IPN

Sample Code	I (a.u.)	Angle of Diffraction at 2Θ-scale	FWHM at 2Θ- scale	Coherence length (Å)
Gr	3258.6	15.66^0	1.87^0	0.77
GrA	23508.6	28.03^0	0.09^0	14.53
GrA-cl-poly(AAm)	2594.8	28.05^0	0.19^0	7.72

Where, Gr = *Gum rosin*; GrA = *Gum rosin* alcohols; GrA-cl-poly(AAm) = crosslinked grafted adsorbent

4.0 Conclusion

The graft copolymer of polyacrylamide chains with reduced *Gum rosin* showed 83% toxic malachite green dye removal from waste water. Pseudo second order kinetics was found to fit well to Langmuir isotherm model. Thus, the synthesized adsorbent was found to be comparable with reported adsorbents in the literature for removal of toxic dyes. However, the present adsorbent being prepared from natural backbone is green in nature and is of great eco-importance.

5.0 Acknowledgment

Authors are highly grateful to MHRD for providing financial assistance to carry out our research work. Authors are also thankful to DST-FIST for providing financial assistance for the procurement of equipment used in the characterization of the samples.

References

1 K. Kabiri, H. Omidian, S. A. Hashemi, M. J. Zohuriaan-Mehr, *Eur. Polym. J.*, 2003, 39, 1341-1348.
2 H. Mittal, B. S. Kaith, R. Jindal, *Adv. Appl. Sci. Res.*, 2010, 1, 56-66.
3 Y. Liu, W. Liu, W. Chen, L. Sun, G. Zhang, *Polym. J.*, 2007, 48, 2665-2671.
4 S. G. Alla, M. Sen, A. W. M. El-Naggara, *Carbohydr. Polym.*, 2012, 89, 478– 485.
5 X. Li, W. Wu, J. Wang, Y. Duan, *Carbohydr. Polym.*, 2006, 66, 473–479.
6 W. Wang, A. Wang, *Carbohydr. Polym.*, 2010, 80, 1028–1036.
7 K. Sharma, B. S. Kaith, V. Kumar, V. Kumar, S. Som, S. Kalia, H.C. Swart, *RSC. Adv.*, 2013, 3, 25830–25839.
8 S. Cai, Y. Hu, X. Zhao, Z. Suo, *J. Appl. Phys.*, 2010, 108, 113514-8.
9 B. Podkoscielna, A. Bartnicki, B. Gawdzik*, eXpress Polym. Lett.,* Vol.6, No.9 (2012) 759–771.
10 B. S. Kaith, Saruchi, R. Jindal, M. S. Bhatti, *Soft Matter*, 2012, 8, 2286-2293.
11 K. S. Soppirnath, T. M. Aminabhavi, *Eur. J. Pharm. Biopharm.*, 2002, 53, 87–98.
12 A. S. Deshmukha, C. M. Setty, A. M. Badiger, K. S. Muralikrishna, *Carbohydr. Polym.*, 2012, 87, 980– 986.
13 B. Singh, N. Sharma, *Carbohydr. Polym.*, 2008, 74, 489–497.
14 C. Chang, B. Duan, J. Cai, L. Zhang, *Eur. Polym. J.*, 2010, 46, 92–100.
15 S. Duran, D. Solpan, O. Guven, *Nucl. Instrum. Methods. Phys. Res. B.*, 1999, 151, 196-199.
16 E. Karada, O. B. Uzum, D. Saraydin, *Eur. Polym. J.*, 2002, 38, 2133–2141.
17 N. B. Milosavljevi, M. D. Risti, A. A. Peri-Gruji, J. M. Filipovi, S. B. Strba, Z. L. J. Rakocevi, M. T. K. Krusi, *Colloids Surf. A: Physicochem. Eng. Aspects*. 2011, 388, 59–69.

18 Y. Zheng, S. Hua, A. Wang, *Desalination*, 2010, 263, 170–175.

19 B. V. Slaughter, S. S. Khurshid, O. Z. Fisher, A. Khademhosseini, N. A. Peppas, *Adv. Mater.*, 2009, 21, 3307–3329.

20 A. I. Raafat, M. Eid, M. B. El-Arnaouty, *Nucl. Instrum. Methods Phys. Res.*, 2012, 283, 71–76.

21 H. A. A. El-Rehim, E. A. Hegazy, H. L. A. El-Mohdy, *J. Appl. Polym. Sci.*, 2004, 93, 1360–1371.

22 Allan S. Hoffman, *Adv. Drug Delivery Rev.*, 2012, 64, 18–23.

23 K. Y. Lee, D. J. Mooney, *Chem. Rev.*, 2001, 101, 1869–1880.

24 K. T. Nguyen, J. L. West, *Biomaterials*, 2002, 23, 4307–4314.

25 D. M. Yebra, S. Kiil, K. D. Johansen, C. Weinell, *Prog. Org. Coat.*, 2005, 53, 256–275.

26 Y. Kumook, *Forensic Sci. Int.* 2008, 176, 111–120.

27 M. Z. N. Xiao-an, W. Y. C. L. Gui-fu, *J. forest prod. ind.*, 2013, 2, 2325 – 4513.

28 X. Liu, W. Xin, J. Zhang, *Green Chem.*, 2009, 11, 1018–1025.

29 P. A. Wilbon, Y. Zheng, K. Yao, C. Tang, *Macromol.*, 2010, 43, 8747–8754.

30 Y. Chen, P. A. Wilbon, Y. P. Chen, J. Zhou, M. Nagarkatti, C. Wang, F. Chu, A. W. Decho, C. Tang, *RSC Adv.*, 2012, 2, 10275-10282.

31 J. Wang, Y. P. Chen, K. Yao, P. A. Wilbon, W. Zhang, L. Ren, J. Zhou, M. Nagarkatti, C. Wang, F. Chu, X. He, A. W. Decho, C. Tang, *Chem. Commun.*, 2012, 48, 916–918.

32 Y. Zheng, K. Yao, J. Lee, D. Chandler, J. Wang, C. Wang, F. Chu, C. Tang, *Macromol.*, 2010, 43, 5922–5924.

33 W. Brostow, H. E. H. Lobland, S. Pal, R. P. Singh, *J. Mater.Edu.*, 2009, 31, 157 – 166.

34 M. Baek, C. O. Ijagbemi, S. O, D. Kim, *J. Hazard. Mater.*, 2010, 176, 820–828.

35 S. R. Shirsath, A. P. Patil, R. Patil, J. B. Naik, P. R. Gogate, S. H. Sonawane, *Ultrason. Sonochem.*, 2013, 20, 914–923.

36 Y. N. Patel, M. P. Patel, *Chin. Chem. Lett.*, 2013, 24, 1005–1007.

37 B. Mandala, S. K. Ray, *Carbohydr. Polym.*, 2013, 98, 257– 269.

38 R. Bhattacharyya, S. K. Ray, *J. Ind. Eng. Chem.*, 2014, 20, 3714–3725.

39 R. Bhattacharyya, S. K. Ray, B. Mandal, *J. Ind. Eng. Chem.*, 2013, 19, 1191–1203.

40 G. Alsenani, *Am. J. Appl. Sci.*, 2014, 11, 1553-1557.

41 K. V. Kumar, *J. Hazard. Mater.*, 2006, 137, 1538–1544.

42 T. M. Elmorsi, *J. Environ. Protect.*, 2011, 2, 817-827.

43 D. J. Alderman, *J. Fish Diseases,* 1985, 8, 289-298.

44 Gregorio Crini, *Bioresour. Technol.*, 2006, 97, 1061-1085.

45 H. Mittal, V. Parashar, S.B. Mishra, A.K. Mishra, *Chem. Eng. J.,* 2014, 255, 471-482.

46 I. Safarik, M. Safarikova, *Water Research*, 2002, 36, 196–200.

47 E. Forgacs, T. Cserhati, G. Oros, *Environ. Int.*, 2004, 30, 953–971.

48 E. Akar, A. Altinisik, Y. Seki, *Ecol., Eng.*, 2013, 52, 19– 27.

49 D. Solpan, S. Duran, M. Torun, *Radiat. Phys. Chem.*, 2008, 77, 447–452

50 S. Li, H. Zhang, J. Feng, R. Xu, X. Liu, *Desalination,* 2011, 280, 95–102.

51 W. Kangwansupamonkon, W. Jitbunpot, S. Kiatkamjornwong, *Polym. Degrad. Stab.,* 2010, 95 1894-1902.

52 P. Li, Siddaramaiah, N. H. Kim, G. H. Yoo, J. H. Lee, *J. Appl. Polym. Sci*., 2009, 111, 1786–1798.

53 X. Yang, L. Ni, *Chem. Eng. J*., 2012, 209 194–200.

54 R. Bhattacharyya, S. K. Ray, B. Mandal, *J. Ind. Eng. Chem*., 2013, 19, 1191–1203.

55 B. S. Kaith, R. Jindal, H. Mittal, K. Kumar, *Der. Chemic. Sinica*., 2010, 1, 44-54.

56 B. S. Kaith, K. Sharma, V. Kumar, V. Kumar, H.C. Swart, S. Kalia, *Vacuum*, 2014, 101, 166-170.

57 B. S. Kaith, R. Sharma, K. Sharma, S. Choudhary, V. Kumar, S.P. Lochab, *Vacuum*, 2015, 111, 73-82.

58 Kashma Sharma, B.S. Kaith, Vijay Kumar, Susheel Kalia, Vinod Kumar, H.C. Swart, *Geoderma*, 2014, 232–234, 45–55.

59 C. P. Sekhar, S. Kalidhasan, V. Rajesh, N. Rajesh, *Chemosphere*, 2009, 77, 842–847.

60 M. J. Iqbal, M. N. Ashiq, *J. Hazard. Mater*., 2007, 139, 57–66.

61 T. Santhia, S. Manonmani, T. Smitha, *J. Hazard. Mater*., 2010, 179, 178–186.

62 S. Ramezani, A. A. Pourbabaee, H. J. Daneshmand, *J. Bioremed. Biodeg.* 2013, 4, 1-6.

63 Saruchi, B. S. Kaith, R. Jindal, V. Kumar, M. S. Bhatti, *RSC Adv*., 2014, 4, 39822–39829.

64 W. Brostow, T. Datashvili, J. Geodakyan, J. Lou, *J. Mater. Sci*., 2011, 46, 2445–2455.

65 Ch. 8 In performance of plastics, Ed. W. Brostow, Hanser, Munich-Chincinnati, 2000.

66 V. H. Orozco, W. Brostow, W. Chonkaew, B. L. Lopez*, Macromol. Symp*., 2009, 277, 69–80.

67 L. Wang, Y. Shi, Y. Wang, H. Zhang, H. Zhou, Y. Wei, S. Tao, T. Ma, *Chem. Commun*., 2014, 50, 1701-1703.

Figure Captions:

Fig. 1 Effect of initial concentration of dye on dye uptake

Fig. 2 Effect of feed concentration on dye uptake

Fig. 3 (a) second order kinetics, (b) intra particle diffusion

Fig. 4 Langmuir isotherm $1/Q_e$ vs $1/C_0$

Fig. 5 The plot of ln K_d vs 1/T for evaluation of standard enthalpy and entropy change

Fig. 6 FTIR spectra of (a) *Gum rosin* acids, (b) *Gum rosin* alcohols, (c) GrA-cl-poly(AAM), (d) Dye adsorbed GrA-cl-poly(AAm)

Fig. 7 SEM images of (a) *Gum rosin* acids, (b) *Gum rosin* alcohols, (c) GrA-cl-poly(AAM)

Fig. 8 X-ray diffraction pattern of (a) *Gum rosin* acids, (b) *Gum rosin* alcohols, (c) GrA-cl-poly(AAM)

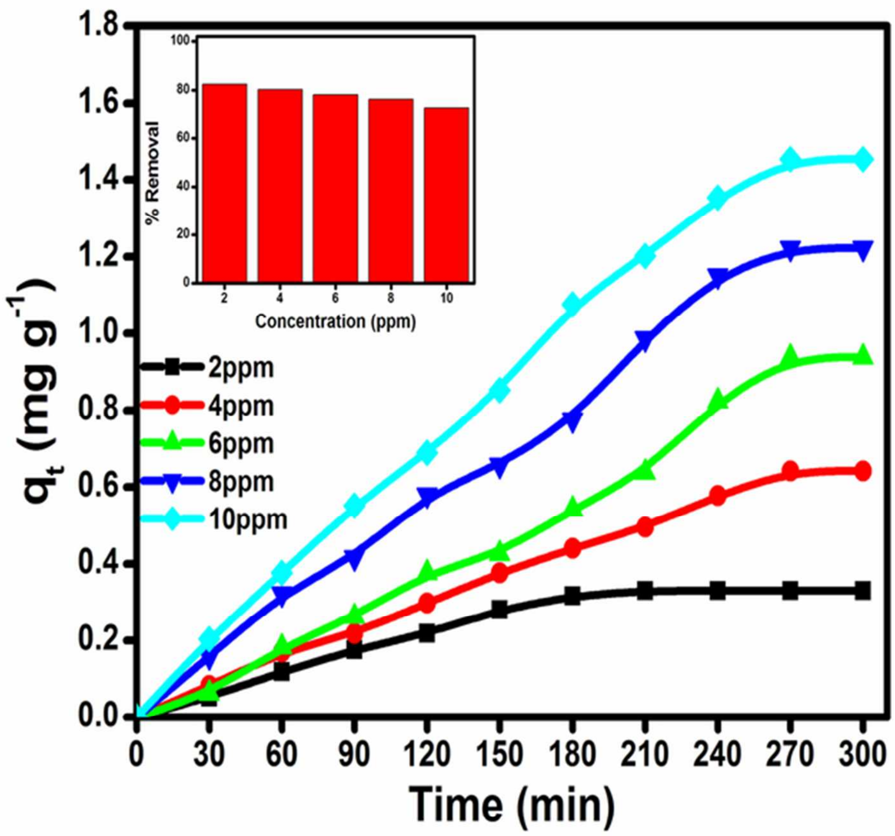

Fig. 1

Fig. 1 Effect of initial concentration of dye on dye uptake
29x29mm (600 x 600 DPI)

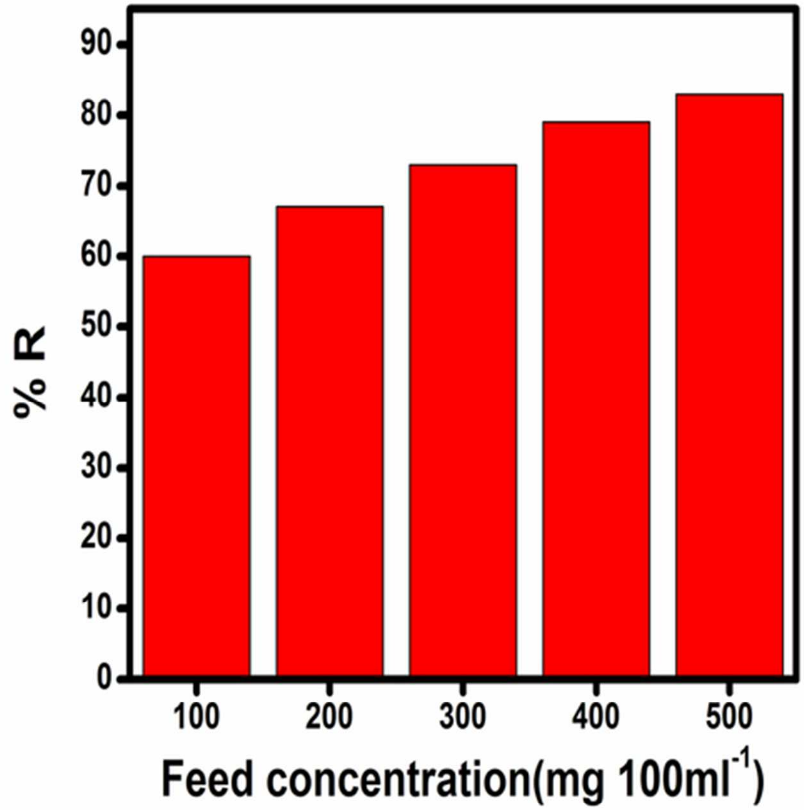

Fig. 2

Fig. 2 Effect of feed concentration on dye uptake
25x25mm (600 x 600 DPI)

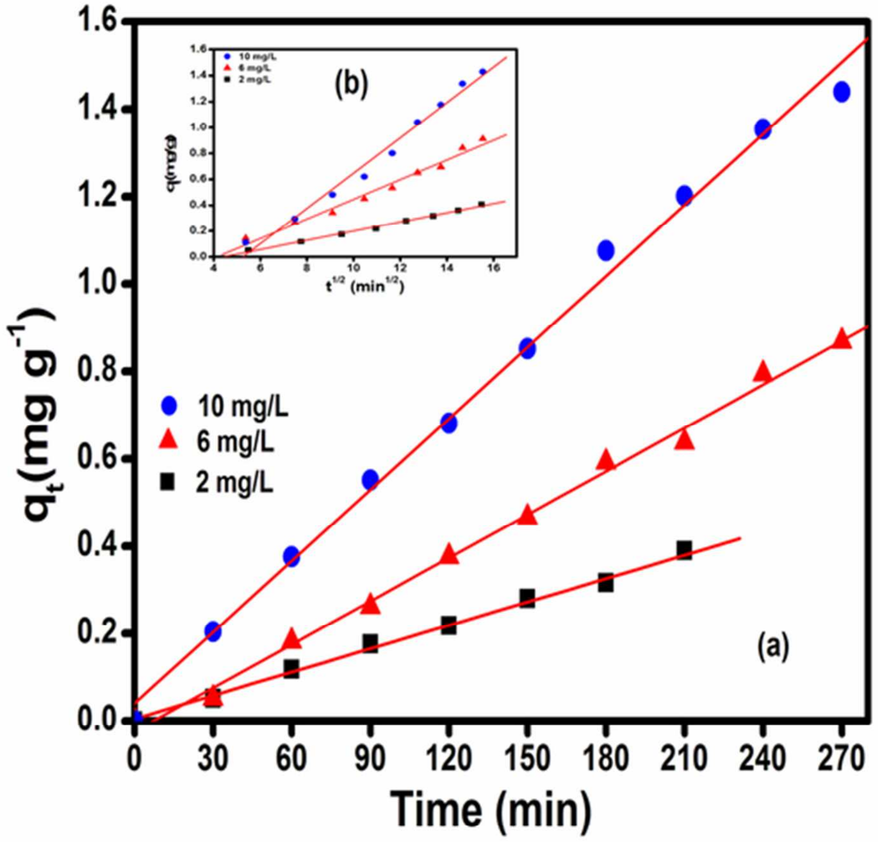

Fig. 3

Fig. 3 (a) second order kinetics, (b) intra particle diffusion
25x25mm (600 x 600 DPI)

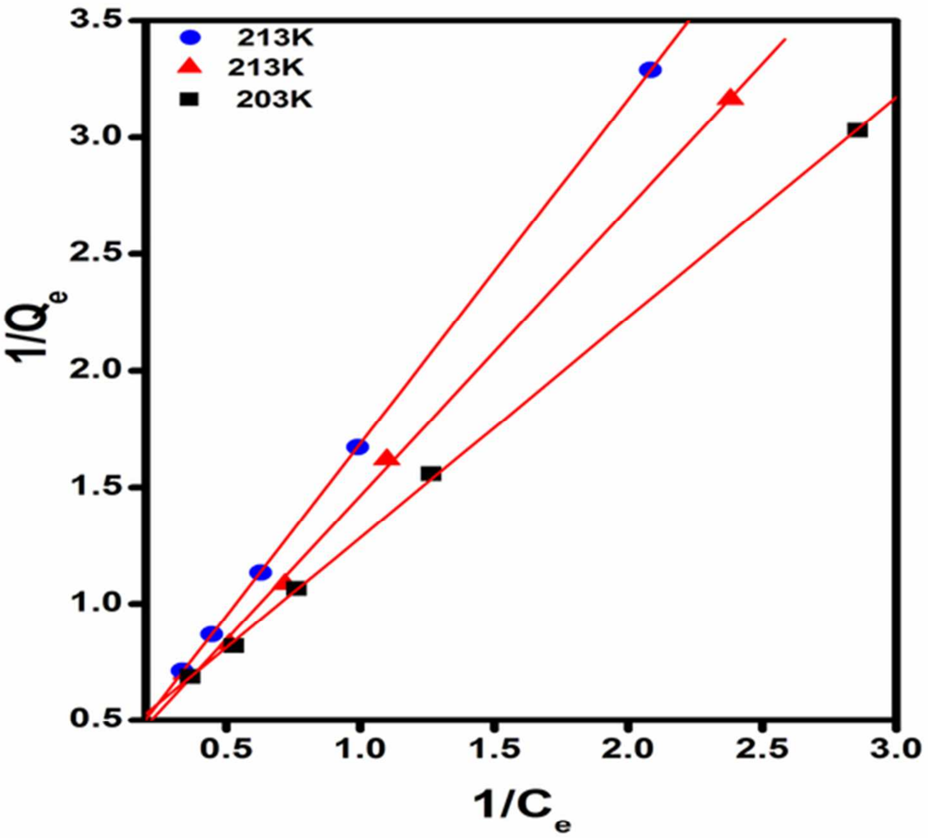

Fig. 4

Fig. 4 Langmuir isotherm 1/Qe vs 1/C0
25x25mm (600 x 600 DPI)

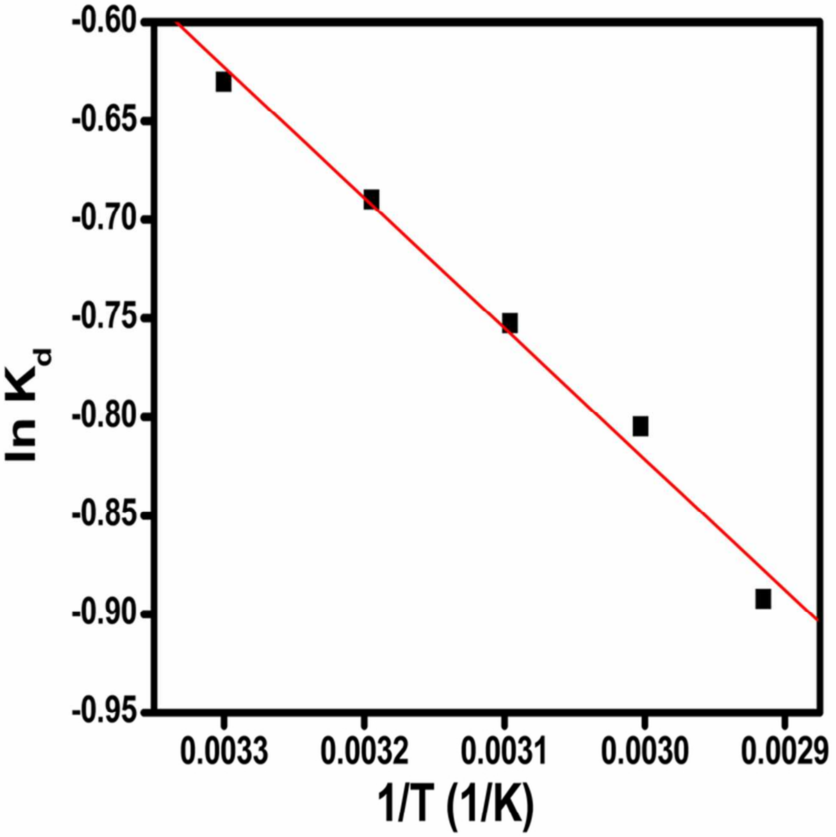

Fig. 5

Fig. 5 The plot of ln Kd vs 1/T for evaluation of standard enthalpy and entropy change
38x38mm (600 x 600 DPI)

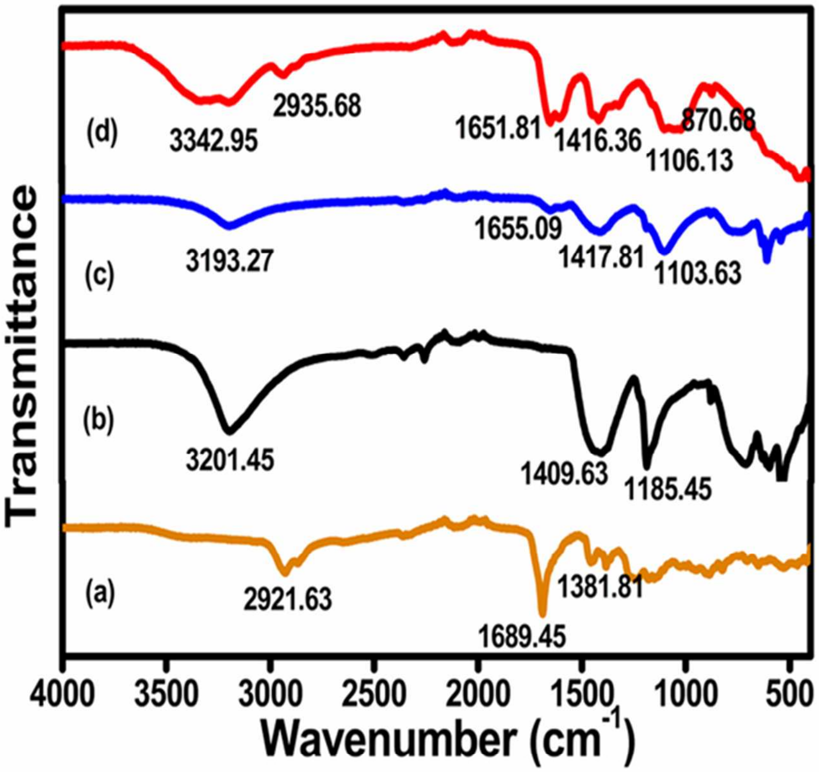

Fig. 6

Fig. 6 FTIR spectra of (a) Gum rosin acids, (b) Gum rosin alcohols, (c) GrA-cl-poly(AAM), (d) Dye adsorbed GrA-cl-poly(AAm)
31x31mm (600 x 600 DPI)

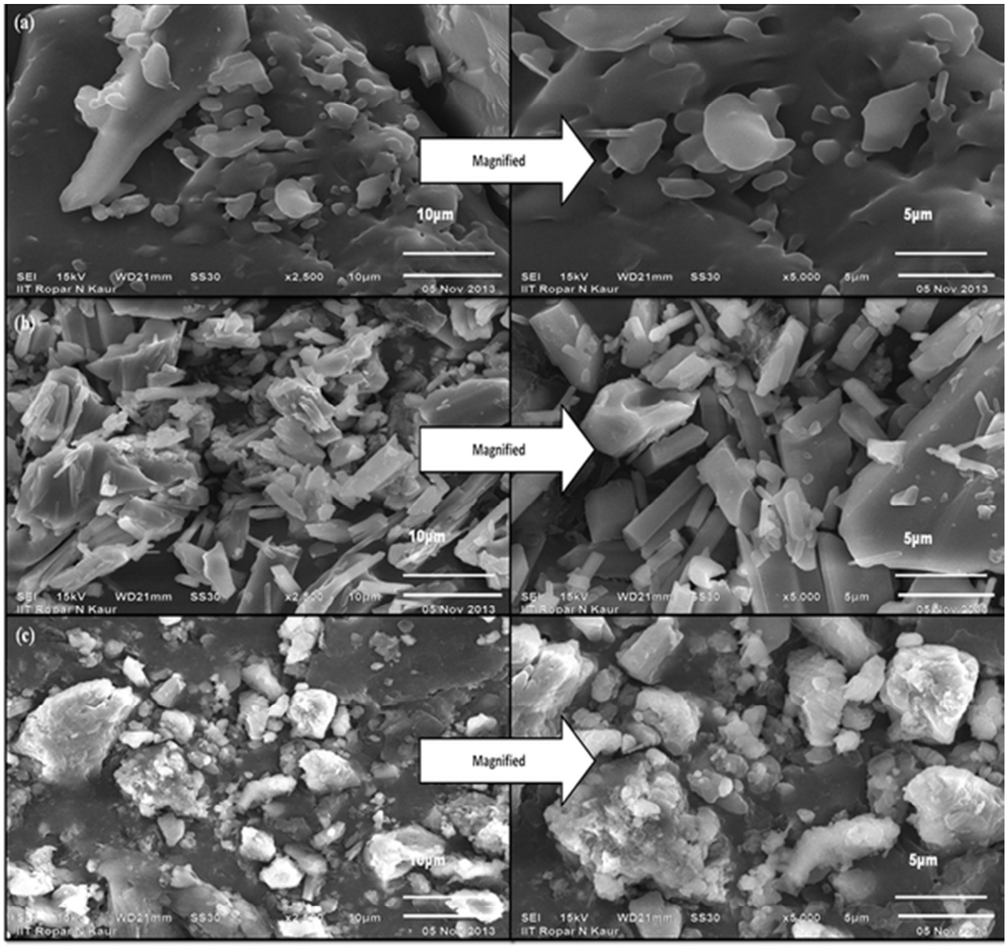

Fig. 7

Fig. 7 SEM images of (a) Gum rosin acids, (b) Gum rosin alcohols, (c) GrA-cl-poly(AAM)
25x25mm (600 x 600 DPI)

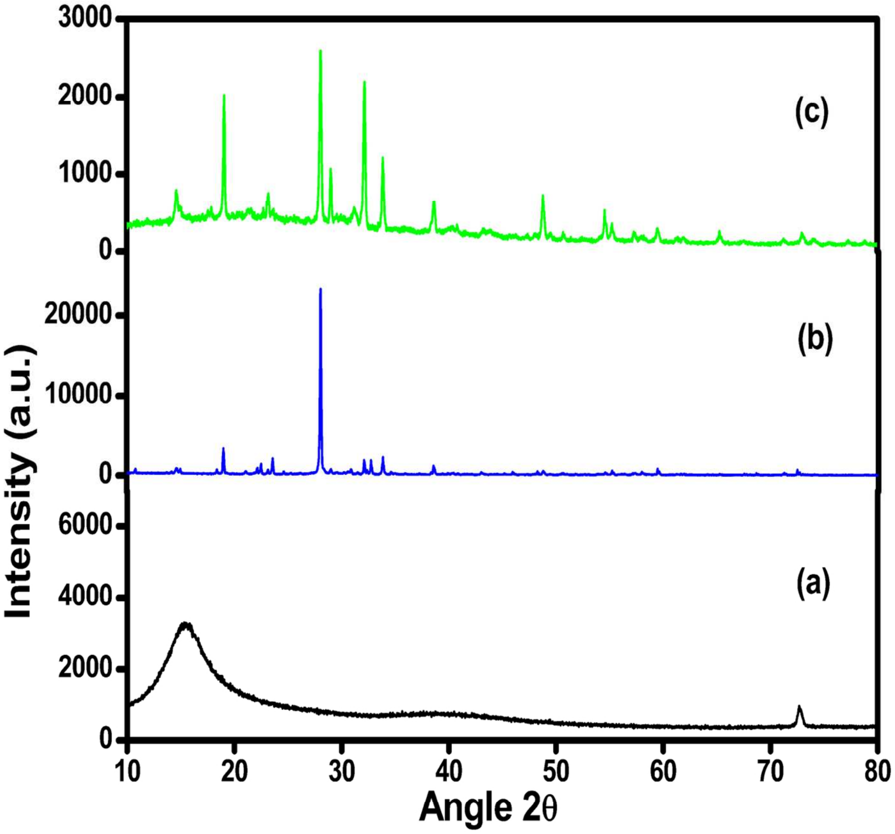

Fig. 8

Fig. 8 X-ray diffraction pattern of (a) Gum rosin acids, (b) Gum rosin alcohols, (c) GrA-cl-poly(AAM)
68x68mm (600 x 600 DPI)